FOI-R--1301--SE
September 2004
ISSN 1650-1942
Scientific report

Björn Montgomerie

Vortex Model for Wind Turbine Loads and Performance Evaluation

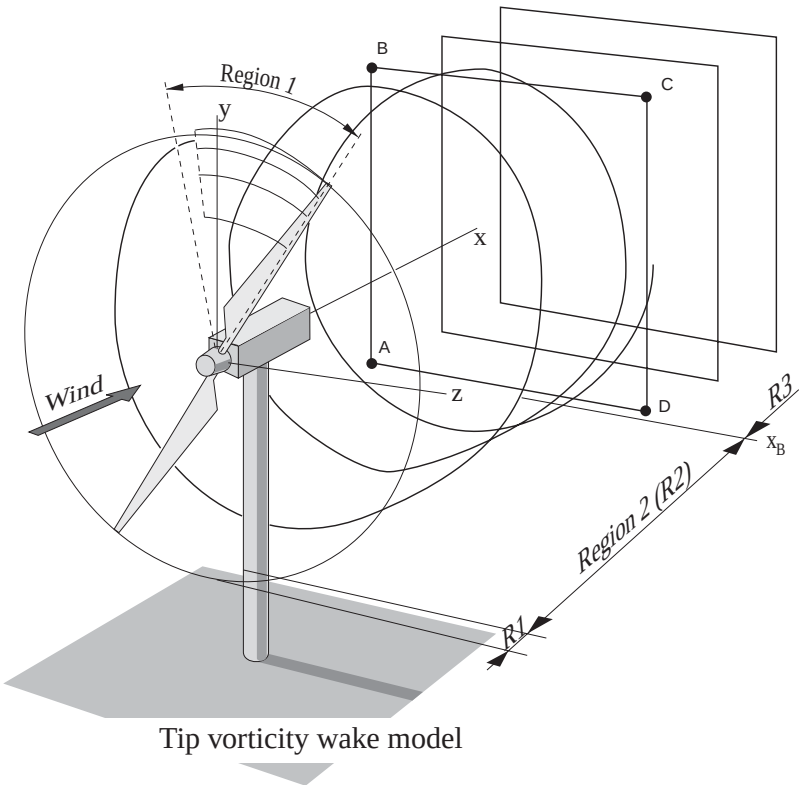

Tip vorticity wake model

SWEDISH DEFENCE RESEARCH AGENCY

Aeronautics, FFA
SE-172 90 Stockholm

FOI-R--1301--SE

September 2004

ISSN 1650-1942

Scientific report

Björn Montgomerie

Vortex Model for Wind Turbine Loads and Performance Evaluation

Issuing organization FOI – Swedish Defence Research Agency Aeronautics, FFA SE-172 90 Stockholm	**Report number, ISRN** FOI-R--1301--SE	**Report type** Scientific report
	Research area code 7. Wind energy	
	Month year September 2004	**Project no.** B827404
	Customers code STEM	
	Sub area code 76 Wind energy	

Author/s (editor/s) Björn Montgomerie	**Project manager** Björn Montgomerie
	Approved by Sven-Erik Thor
	Sponsoring agency Swedish Energy Agency
	Scientifically and technically responsible Björn Montgomerie

Report title

Vortex Model for Wind Turbine Loads and Performance Evaluation

Abstract

Vortex theory is used to form a basis for calculation of the deceleration of the flow through a wind turbine rotor or the acceleration of this flow through a propeller disk. Advice for practical application of the trailing vortex sheet concentration, behind the blades, is given.

This report is to be considered a draft report whose finishing touches and numerical methods consequences are still missing due to lack of continued funding.

Keywords

wind, turbine, aerodynamics, Himmelskamp

Further bibliographic information	**Language** English
ISSN 1650-1942	**Number of pages:** 27
	Price acc. to pricelist

Utgivare Totalförsvarets Forskningsinstitut - FOI Flygteknik FFA 172 90 Stockholm	**Rapportnummer, ISRN** FOI-R--1301--SE	**Klassificering** Vetenskaplig rapport
	Forskningsområde Flygteknik	
	Månad, år September 2004	**Projektnummer** B827404
	Verksamhetsgren Flygteknisk forskning	
	Delområde Vindenergi	
Författare/redaktör Björn Montgomerie	**Projektledare** Björn Montgomerie	
	Godkänd av Sven-Erik Thor	
	Uppdragsgivare/kundbeteckning Energimyndigheten	
	Tekniskt och/eller vetenskapligt ansvarig Björn Montgomerie	
Rapportens titel (i översättning) Virvelmodell för utvärdering av vindturbinlaster och prestanda		

Sammanfattning

Vortex theory is used to form a basis for calculation of the deceleration of the flow through a wind turbine rotor or the acceleration of this flow through a propeller disk. Advice for practical application of the trailing vortex sheet concentration, behind the blades, is given.

Virvelteori används i denna rapport för att grundlägga en praktisk metod för beräkning av uppbromsningen genom en vindturbin. Teorin kan också användas för propellrar där emellertid vinden accelereras snarare än bromsas. Råd för lämplig metodik till koncentration av den bakom bladen avgående virvelmattan ges. Vidare diskuteras hur lämpliga mätningar kan tillföra metoden ökad noggrannhet.
Denna text är ett ofärdigt rapportutkast som saknar en noggrann kontrolläsning samt en återmatning från numeriska experiment enligt den beskrivna metodiken. Rapporten ska därför ses som en första iteration mot en metod.

Nyckelord

vindturbin, aerodynamik, virvel, last, prestanda

Övriga bibliografiska uppgifter	**Språk** Engelska
ISSN 1650-1942	**Antal sidor:** 27
Distribution enligt missiv	**Pris: Enligt prislista**

SUMMARY

This memo is a proposal for an improved aerodynamic method for prediction of external loads and performance of a wind turbine. The key elements in the model are the radial subdivision of the blade into elements and the use of vortex-induction methods. The former provide the load on the element. The latter provides the prerequisites for the blade element load calculation. To round out the description, the two methods are parts of one coherent method and the one can not do without the other. The acronym BEI is proposed for the Blade Element Induction methods.

The text includes descriptions of essential elements of the model as well as some advice for testing in order to support the model development. The model is of the "Engineering" type, i.e. it is useful in the context of wind turbine aeroelastic simulation. This requires that the model is relatively fast. Such a model is typically several orders of magnitude faster than e.g. Computer Fluid Dynamics (CFD) models. Presently several engineering models for the same purpose include the Blade Element Momentum (BEM) technique, which is well known by scientists and engineers with any relation to wind turbine performance theory. The BEM technique can be used to create very rapid computer code. The BEI technique can be thought of as being somewhere in between CFD and BEM. It is more accurate than BEM. Its accuracy in relation to CFD can hardly be given because not sufficient experience has been had at this date.

The model as described here is given with the hope that a maturing computer program based on the ideas will contribute to better predictions of the loads and performance behavior of the future very large wind turbines, which are now emerging. Accuracy in the design stage becomes increasingly more important the larger the machine is. Support, in this respect, is also coming from the increasing speeds of computers.

Unfortunately it was not possible to find funding for a continuation of the project, in which this report was written. The original hope was that experience with a computer program based on the theory developed herein would have been available at the time of reporting. The experience from such a program code is of course extremely valuable for improving the theory and numerical accuracy of the results. In this type of applied research the method always includes development of theory and its application in an iterative way, which converges toward a reliable computer code for accurate results. No such code seems likely to appear in the foreseeable future.

CONTENTS

1. INTRODUCTION …… 9
2. BLADE LOADING MODEL …….. 9
3. VORTEX MODEL …….. 9
    3.1 General …… 9
    3.2 Vorticity Regions …… 10
    3.3 Economizing the Induction Calculations …… 11
4. CONCENTRATION OF VORTICITY …… 12
    4.1 Determining the Radial Position from which Concentrated Vortices Emanate ……. 12
    4.2 Vortex concentration behind a wing …….. 12
    4.3. The Weighting Method - A Different Method of Finding b´ …… 14
    4.4.Exploratory Test ……. 14
5. PROPAGATION OF CONCENTRATED VORTICITY …… 15
6. PREPARATIONS FOR A COMPUTER CODE ALGORITHM …… 17
7. INTERFACING WITH AERFORCE …… 18
8. TRIMMING THE MODEL USING EXPERIMENTS ……. 18
    8.1General Model Parameter - Needs for Trimming …….. 18
    8.2 Finding the Angle of Attack in Testing ……. 18
9. REFERENCES …… 21
Appendix – Flow Disturbance from a Two-dimensional Solid Body …… 23

1. INTRODUCTION

This text deals with the construction of an aerodynamic model to deal with the loads on a wind turbine rotor. The model is set up with the purpose of computer implementation. The typical state-of-the-art approach is to apply the well known steady flow Blade Element Momentum (BEM) method together with its many additions to account for flows that are time variable. Here the alternative path offered by vortex and induction theory is applied. Induction theory can be coupled with blade element theory thus eliminating the need for stream tube momentum balance with thrust. It is proposed that the notation Blade Element Induction (BEI) is used. The advantages of BEI over BEM is the inherent capability in BEI to handle all kinds of dynamic events. It is not necessary to apply "fixes" to patch up the BEM method to act as a dynamic method. Another advantage is that the calculated inflow distribution accuracy of the induction methods is higher according to converging conclusions from several sources of information. The main reason for not having used BEI in favour of BEM is that BEI is more time consuming. Recent and ongoing advances, in computer capabilities, are changing the foundation for the validity of past decisions in this respect. Moreover, proper modeling can be geared toward calculation efficiency as well. The latter topic is addressed in this text as well.

There are several descriptions in the literature where BEI is applied with iteration to satisfy a balance between the strength of the circulation distribution on the blades and the disk inflow. Such a method, without modifications, does not apply in a context where any dynamic elements can be identified.

In the presently proposed BEI model, at every time step of a simulation, the flow situation, on the individual blade element, is allowed to give rise to a small trailing vortex element which couples geometrically to the previously created ditto. The transport velocity of these vortices (one on either side of the blade element) is in principle effectuated by the free stream velocity and the induction from all other participating vortex elements. The velocity vector, at each vortex element, is then multiplied by the size of the chosen time step. Should a steady and polar symmetric case be studied, the steady solution will be asymptotically approached from a start condition with no induction. Therefore the time simulation method can be used also for performance point evaluation.

2. BLADE LOADING MODEL

The present method requires the problem of force calculation on the blade elements to have been solved separately. The approach has been to use two-dimensional (2D) aerodynamic coefficients tabled in an input file. Between points given the coefficients are interpolated for angle of attack. The local velocity vector together with the local blade twist/pitch gives the angle of attack to be applied. The angle of attack is used to interpolate in the tables for the aerodynamic coefficients for lift, drag and moment. Lately an adaptation from 2D to 3D has been applied, by several workers in the field, before a calculation of loads or performance is carried out. The rest of the technique is, however, identical to the one described. The 2D to 3D adaptation is a whole science in its own right and it is not dealt with here.

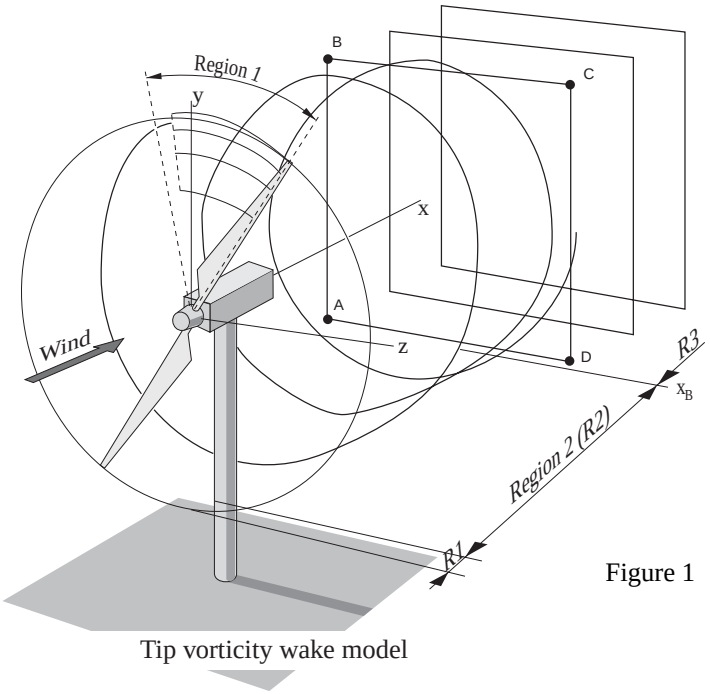

Figure 1 Tip vorticity wake model

3. VORTEX MODEL

3.1 General

A so called free vortex model constitutes the intellectual entry into the world of vortex modeling. In a free vortex model all vortex elements affect all other vortex elements. As a result a self-development occurs in the vortex system displacement. This is most visible as a transportation of the vortices downstream. However, nature does not follow the law of induction, for potential flows, according to the French scientists Biot and Savart although their law has been exclusively used in several computer models of wind turbine flows. (Their intent was originally to apply the law in the field of electricity.) In reality the viscous effects cause the development of the vortex system to deviate considerably from that of a free wake model.

One prominent feature of reality is to concentrate the trailing vorticity from the blades into distinct tip vortices, one for each blade tip. The concentration seems to occur very rapidly. Photographic evidence from smoke/vortex visualization indicates complete rollup, of the trailing vortex sheet, within 20 degrees of azimuth travel. Although visible rollup seems to be the case when smoke injected flows are studied in photographs, there are indications that some stray vorticity survives outside the tip vortex and that the circulation of the tip vortex decreases with age. For modeling purposes it may be important to receive high quality data from well designed tests such as the European project MEXICO (Ref. 8) where a thorough flow field mapping is in the planning. The corresponding trailing vorticity that should be expected to come from the root of the blade is not well captured in photographs. The root vorticity can therefore be assumed to be more diffuse although very much present as some load cases have shown (without smoke). In calculation the concentration, from vortex sheet to single vortex, does not occur when the Biot-Savart (BS) law is applied without modification. The BS law is strictly only applicable to potential flows. Also the tip vortex spiral does not travel downstream with the radius and pitch that pure BS calculation gives as a result. A few tricks of the trade are necessary as additions to the pure BS law application, see Sect. 4 and 5 for radius and pitch modification of tip vortices.

3.2 Vorticity Regions

The computer time required for BEI is considerably higher than that of BEM. This calls for some inventiveness in reducing the total free wake description in terms of number of vortex elements. Vortex elements are modeled to be a piece of straight line confined between the end points. The latter are referred to as *nodes*. The following features supporting this need are suitably implemented in an efficient model.

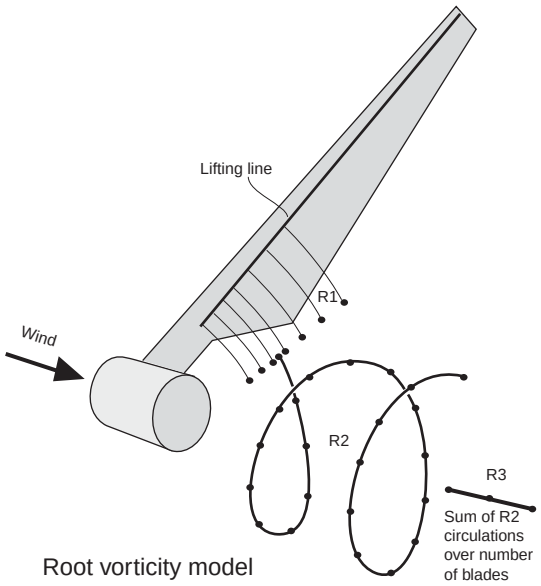

Figure 2

Region 1

The fine representation of the trailing vorticity filaments in Region 1 (R2) is necessary for smooth induction on the lifting line (LL) representation of the blade. It should be assumed that the model is implemented in computer code. In such code the simulation occurs through incremental time steps. For each time step every discrete trailing filament is furnished with a "newborn" contribution behind the lifting line. At the same time step the oldest members of the R2 filaments vanish from R2, are grouped together as newborn tip and root vortex elements in R2. The R2 vorticity is closest to the lifting line. It therefore has the greatest influence on the blade. Because of its very short extent into the wake its geometrical characteristics can be prescribed according to prior knowledge of such shapes. That knowledge can be had from experiments. If prescription is used then great savings in computer time can be accomplished with marginal sacrifice of accuracy.

Furthermore, the time variation of the circumstances at the lifting line can be allowed also to generate shed vortex filaments (parallel to the LL). If these filaments are used exclusively to induce on the lifting line and not in the rest of the vortex system, a reasonable balance between accuracy and calculation expediency is achieved. This particular induction is used together with indicial theory in the spirit of Wagner and Küssner, see e.g. Ref. 3. The consequence is a simulation of the potential flow unsteady aerodynamic effects in the loading of the blade. The presently used method is to implement 2D profile behavior in response to variable aerodynamic circumstances. However, the regions near the root and near the tip will then exaggerate the effect while the indicial response method would better represent the 3D real effects. This can be explained using the simple thought that, at the end of a semi-finite wing, induction effects will be exactly one half of the 2D effect. Since the proposed model has inducing vorticity only where it belongs (not going to infinity) the induction will be correctly evaluated and therefore the consequential loading will be correct.

The utilization of shed vorticity in this respect has been explored in Refs. 1 and 2 with demonstrated significant differences between the 2D approach and the 3D indicial approach. The possibility of application of the indicial method is mentioned here but its model consequences will not be further pursued in this text. It is assumed that the 2D unsteady aerodynamic methods will be available in the application of the blade element aerodynamics.

Region 2

Mostly a convex circulation distribution makes up the pretext for the trailing vorticity. Vortices with the same sense of rotation are concentrated into one vortex as indicated in Fig. 3.

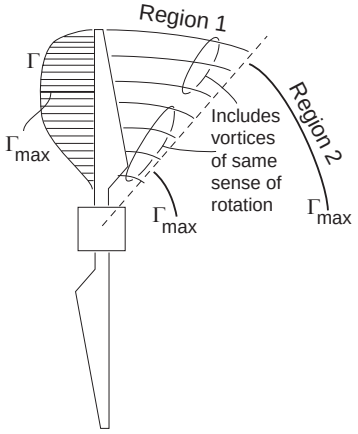

Figure 3 – Normal circulation distribution

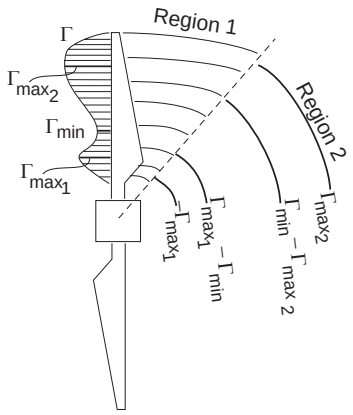

Figure 4 – Double hump distribution

The concentrated vortices from the tip and the root reflect the normal behavior of wakes. Here Region 2 may end at different downstream positions for tip and root vortices. It should be noted that, although the root vortex is not apparent in smoke visualization, it nevertheless exists and the most adequate model is using concentrated vortices in R2. The R2 vortices may be modeled to account for the complication that more than two spirals per blade appear in the flow. This situation occurs when the blade circulation distribution portrays a double hump circulation distribution as sketched in Fig. 4. Real world experience of such flows was reported from studies of the NREL tests, see Ref. 4. If these effects are modeled also then there is a need for four definitions of the R2 region, one for each vortex.

The strength of the R2 vortices equals the sum of the corresponding R2 vortices per blade. The corresponding vortices are those that have the same sense of rotation. The radial position of the R2 concentrated vortex is obtained from the center of gravity of the R2 vortices according to Sect. 4.

Region 3
The far wake causes typically only 10% of the induction on the rotor. For this reason a cruder description can be accepted without degrading the accuracy too much. It is proposed that this part of the wake be represented by closed “circular” vortex filaments with the very crude approximation of using only four points, thus replacing the tip spirals with square filaments, see Fig. 1. For each full revolution of the rotor a new R3 square is born – provided the simulation is old enough to have reached a mature R2 length. The square represents the tip vortex from one blade. Its birth velocity vector at the center is maintained throughout the life time of the square. Its shape is not deformed but maintains its birth time tilt and yaw position.

The corresponding root vortex is modeled as a concentrated line in the center of the wake. Its strength is the sum of the strength of the concentrated root vortices from R2. As mentioned, its R2/R3 border must not coincide with that of outer radius R2 filaments.

The induction from the region is only used for evaluation at the blades. Thus, no induction on the R1 or R2 vortex nodes need be considered.

3.3 Economizing the Induction Calculations
The modeling, according to the region definition above, indicates features which reduce the calculation time in relation to a full free wake approach. Several other concerns encompass the interrelationships between the different regions. It will be shown how each node can be assigned different characteristics, which govern the details of the induction calculations during a computer time simulation. The saving of induction evaluations should be seen in the light of the square law. Thus, if all participating vortex filaments are used to evaluate the induction on all participating filaments, as in a full free wake method, then the calculation time will be approximately proportional to the number of nodes squared.

In R2 it is acceptable to prescribe the shape of all filaments. This can be done using the induction along the blade continuously. This method requires in principle a full induction calculation (no prescription) to be carried out as a preprocessing event either at time of development of the code or as an initial procedure at the beginning of a simulation run. However, shortcuts can be employed.

A good estimate of the influence of the induction on the blade is to say that the vector sum of the induced and the free stream vectors together with the revolutional travel of the blade provide the necessary base from which a simple geometrical algorithm will predict the R2 vortex filament geometry. Since the induction on the blade is calculated for this purpose, then this velocity will be applied throughout R2. This represents the approximation that the induction on the blade (in fact the induction on the line representation of the blade) is equal to the induction on each of the R2 filaments at the same radius. The approximation is good at a mid-position on the blade because the so called tip correction is a factor near 1.0. The approximation is also best closest to the blade. Far from the blade (at say the last nodes of R2) and at the tip the approximation is the worst. In this region it is perhaps best to select an extra point (rotating with the blade) for induction evaluation to improve the accuracy. One consequence of the method is that the position accuracy of the R2 nodes increases when the R2 azimuth region decreases. But, a decreasing R2 region decreases accuracy of the induction on the blade. Generally several numerical experiments will need to be carried out in the development of the code.

With a prescription of the R2 node positions no induction evaluation is necessary in these points. The vortex filament elements between these nodes, however, are used for induction calculation at many other nodes. Exactly which nodes, will become a result of the continued philosophy on this matter.

In R2 induction will be evaluated at several but not all points. The economizing feature is to use the induction at point i and point i+m per filament. These induction velocities are used to move the points accordingly (free stream velocity + induced velocity times the time step). For the points in between, a linear interpolation will give an approximation for the induced velocities. This makes it possible to move the interpolated points also. It will become of interest to know the size of m. It should be judged from the viewpoint of the corresponding azimuth angle travel. It is proposed to let m be a model parameter, which can be varied in numerical exploration when the program is being developed.

4. CONCENTRATION OF VORTICITY

4.1 Determining the Radial Position from which Concentrated Vortices Emanate

The flow through the turbine disk will cause a vorticity sheet to leave the blade/wing trailing edge. In the model it will be artificially concentrated into discrete vortices. One vortex will emanate from the tip, the other from the root end of the blade as described above. The concentration mechanism is most easily analyzed in the flow behind a fixed wing. Therefore, some basic features of airplane wings will be presented to support an important piece of calculation in the proposed model. This is the algorithm for finding the radial coordinate from which the tip vortex should emanate.

4.2 Vortex concentration behind a wing

From a number of text books (E.g. Ref. 6) on the topic it is known that a lifting line bound vortex, which has elliptical distribution, gives rise to a concentrated vortex behind each wing tip. The position is, however, not exactly behind the tip but rather at a certain inboard location. This location is calculated from the simple expression that follows.

$$L = \rho V \int_{-\frac{b}{2}}^{+\frac{b}{2}} \Gamma(y)dy = \rho V \cdot \Gamma_{\max} \frac{\pi}{4} b \quad (1)$$

For elliptical distributions and other distributions the distance between the trailing vortices is obtained from the following mind model.

An imaginary wing is created whose bound circulation distribution has the constant value Γ_{max}. This wing is to have the same total lift L as the real wing. Furthermore it has the same distance between the trailing vortices as its span. This model arises from a more rigorous approach where lift on the wing must correspond to the

downward directed momentum flux infinitely far behind the wing. Alternately it can be expressed as follows:

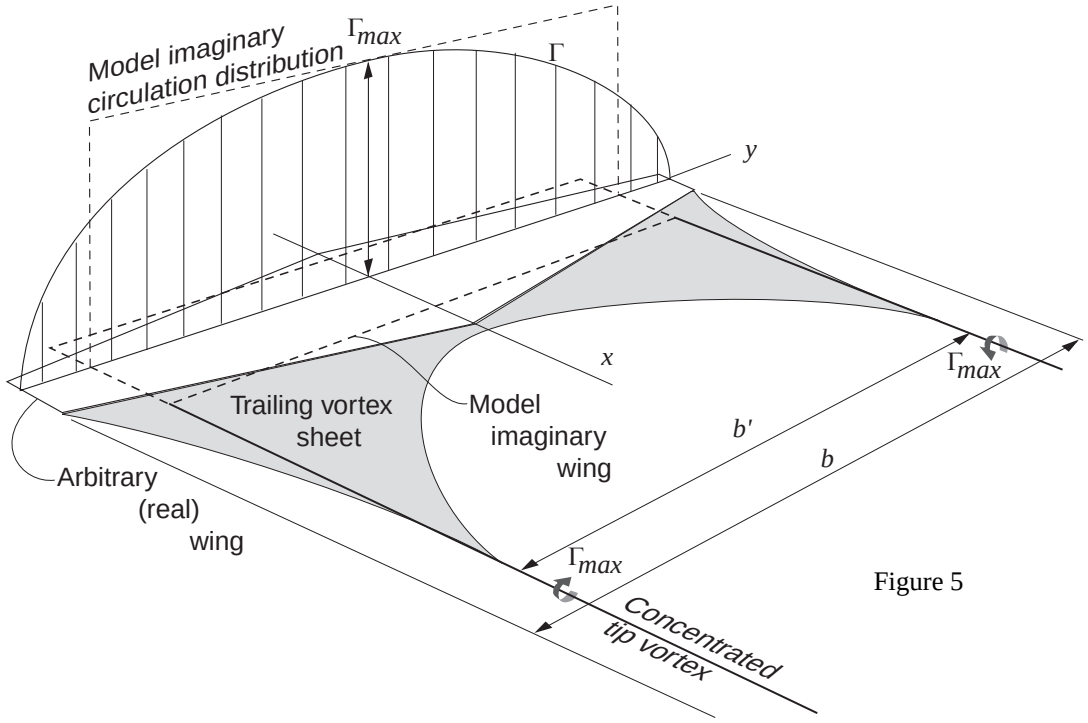

Figure 5

Lift equals the new mass flow, penetrating the Trefftz plane, being deflected downward, multiplied by the downward velocity. It should be noted that the downward velocity is variable within the plane. Expressing the balance mathematically we get

$$L = -\rho V \iint_{\substack{Trefftz \\ plane}} w_\infty \, dydz \qquad (2)$$

In Trefftz plane, infinitely far behind the wing, flow circumstances of interest are purely two-dimensional. The two trailing vortices appear as two two-dimensional potential flow circulation points whose compound induction velocities in the Trefftz plane become

$$w_\infty = -\frac{\Gamma_0}{2\pi}\left\{\frac{\frac{b'}{2}+y}{\left(\frac{b'}{2}+y\right)^2+z^2}+\frac{\frac{b'}{2}-y}{\left(\frac{b'}{2}-y\right)^2+z^2}\right\} \qquad (3)$$

where the *z* coordinate is the vertical coordinate, positive up.

The lift from a constant circulation distribution over the length *b*', of strength Γ_{max} , or the lift obtained after insertion of (3) in (2) is

$$L = \Gamma_{max} b' \rho V \qquad (4)$$

whence generally

$$b' = \frac{L}{\Gamma_{max}\rho V} \qquad (5)$$

For the particular case of the elliptical circulation distribution, identification of the length quantity in (1) and (4) gives

$$b' = \frac{\pi}{4} b \qquad (6)$$

Eqs. (1) and (4) are valid for elliptical distributions only. Eqs. (2), (3) and (5) are valid for general distributions (within the limitations of the theory). In order for the basic assumptions to be valid there must not be a local trough in the circulation distribution. Rather the distribution should be convex between the wing tips.

4.3. The Weighting Method - A Different Method of Finding *b´*

The following thoughts are developed to pave the way for the more complex flow description valid for the vortex flow behind a turbine or a propeller. In the following the word "turbine" mostly also includes propellers, unless specifically noted.

The turbine vortex system, which physically should be thought of as a vortex sheet leaving the trailing edge of the blade, is initially a homogeneous sheet, which rolls up into a concentrated vortex, at least behind the tips. At the root it may not lead to concentration. The continuous sheet must be dealt with using a discrete vortex model for computer calculation purposes. This need enforces the formulation and definition of blade elements whose purpose is to represent local aerodynamic forces and the circulation strength of the vortex that trails from the element. The neighboring elements produce vortices likewise. Since reality creates a concentrated vortex very rapidly, say within 90 degrees of rotor azimuth angle travel, this must be mimicked in simulation. The sketch in Fig. 6 shows the idea but it is not indicative of the computer model, which is described in figures 3 and 4.

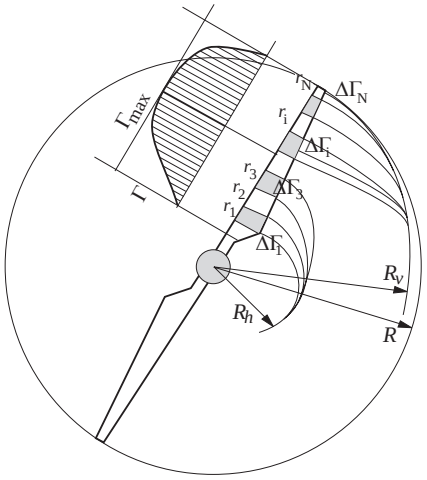

Figure 6

One ingredient in the modeling is to determine the circulation strength of the concentrated vortex. The simulation method will include a simple summation of the circulation value from each elemental vortex that participates in the concentration process. This decision comes from the theorem for constancy of circulation.

For determination of the radius to which all elemental vortices are to travel there is no given simple method. So, an idea must be developed and tested. The idea is to let the circulation strengths of the vortices, which are to be merged, be used as weight coefficients. This is in fact the formula for creating an average. In mathematical terms this idea becomes:

$$R_v = \frac{1}{\Gamma_{Sum}} \sum r_i \Delta\Gamma_i \qquad (7)$$

where

$$\Gamma_{Sum} = \sum \Delta\Gamma_i = \Gamma_{\max} \qquad (8)$$

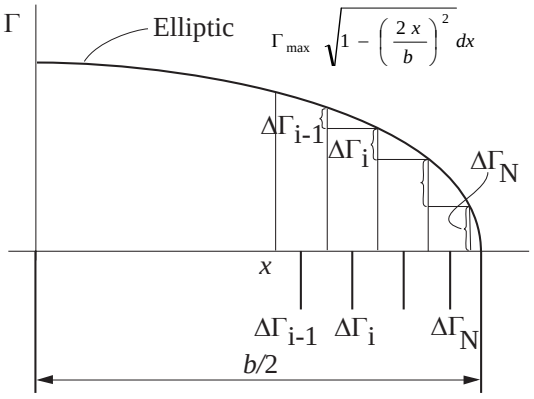

Figure 7

The idea is sketched in Fig. 6, which also shows a similar idea for the hub vorticity.

4.4.Exploratory Test

The idea, embodied in Eqs. (7) and (8), needs to be tested in order to see if this is a reasonable assumption. To find out, the method is applied to the simple non-rotating wing case where the circulation distribution is elliptical.

This allows an analytical solution, for this particular case, as follows.

$$d\Gamma = \Gamma_{\max}\frac{d}{dx}\sqrt{1-\left(\frac{2x}{b}\right)^2}\,dx = \Gamma_{\max}\frac{4x/b^2}{\sqrt{1-\left(\frac{2x}{b}\right)^2}}\,dx \qquad (9)$$

$$x_v = \frac{1}{\Gamma_{\max}}\int_{x_{\max}}^{b/2} x\,d\Gamma = \int_0^{b/2}\frac{(2x/b)^2}{\sqrt{1-\left(\frac{2x}{b}\right)^2}}dx = \frac{b}{2}\int_0^1\frac{\xi^2}{\sqrt{1-\xi^2}}d\xi = \frac{b}{2}\cdot\frac{\pi}{4} \qquad (10)$$

Eq. (9) is a development of Eq. (7) and Eq. (10) is an analytical evaluation of Eq. (7). It is seen that the final result is identically the same proportion of the wing half span as obtained from classical analysis according to Eq. (6). This promising result suggests that the method behind Eq. (7) can be applied in practical implementation for tip and root, even when the blade rotates, albeit it is strictly not a scientific derivation of the proposed method. It is adopted as a practical approximate method for lack of an alternative. A further extension to the validity of this method is to apply it even for the radial range between humps of the type depicted in Fig. 4.

5. PROPAGATION OF CONCENTRATED VORTICITY

There is a significant difference between a rotating blade and a non-rotating wing in that the vortex trailing from the tip of the blade immediately starts traveling toward an increasing radius while the wing tip vortex stays at a constant span *b*'. This difference needs a sub-model of its own. The available perspective is the Biot-Savart theoretical induction and observation of the vortex behavior in testing. As found in Ref. 7 there is a significant difference between the pure inductive behavior from the Biot-Savart law (BS) and that found in testing. Pure BS induction gives a vortex spiral whose radius rapidly increases and whose pitch rapidly decreases. The tests (Ref. 7) show a spiral that has very nearly linearly increasing radius while the pitch is close to constant. Since application of induction is necessary to some extent and the experimental results show differently, the problem becomes to reconcile these different behaviors. To do so the following rules are proposed.

Rules for the calculation mechanism in simulation of the convection vectors:

1. Calculate the maximum circulation strength Γ_{max} at r_{max}, see Fig. 7.
2. Identify the radial position on the blade where the circulation is the greatest. Call it r_{max}!
3. The trailing vortices on the outer side (toward the tip) are treated separately from those on the root side. The latter are concentrated following the same rule as that for the tip vorticity (although real flows do not concentrate).
4. The concentration may take place suddenly after a preset azimuthal angle. The idealized view of Fig. 7 is then not simulated directly. The sudden collection of vortex lines, at the preset azimuth angle, is judged to cause a very small difference from the results of a model that faithfully would simulate the smooth concentration. The concentrated vortex is given its radial position according to the weighting method of Sect. 4.3.
5. The trailing vortex segments, before and after concentration, which are successively generated during the time step simulation, are subject to several convection rules. There is prescription of a velocity vector field, which is superimposed on the induction velocity field using the Biot-Savart law. In addition there is also a reduction of the axial induction, designed to account for the turbulent mixing between the wake stream tube and the ambient air. The latter may be manipulated by a set of multipliers C_{ij}. The following mathematical statements govern and explain the use of these ideas.

An "induced" velocity vector in 3D space will be calculated from

$$\begin{Bmatrix} v_x \\ v_y \\ v_z \end{Bmatrix} = \begin{bmatrix} C_{11} & 0 & 0 \\ 0 & C_{22} & 0 \\ 0 & 0 & C_{33} \end{bmatrix}\left\{\begin{Bmatrix} vp_x \\ vp_y \\ vp_z \end{Bmatrix} + \begin{Bmatrix} vBS_x \\ vBS_y \\ vBS_z \end{Bmatrix}\right\} \qquad (11)$$

which alternatively can be more compactly written

$$\mathbf{v} = [\mathbf{C}]\{\mathbf{vp} + \mathbf{vBS}\} \qquad (12)$$

where

v = Resulting "induced" velocity (later to be added to the free stream velocity)
vp = Prescribed vector (based on analysis of measurements) – details below
vBS = Pure Biot-Savart induction vector from all participating vortex segments
C = Tuning factors on the induced velocity. Its components will typically tend to zero far back in the wake to reflect the diffusion of the structured vortices. Suitable initial default values could be C11=C22=C33=1.0.

The technique proposed in the five points above is to be active throughout the life of a trailing vortex segment. Thus, the Biot-Savart (BS) co-acts with the artificial concentration of the discrete vortex representation. With this in view and the need to adapt to measured results, the numerical values of the quantities in Eqs. (11) and (12) must be estimated. This need calls for another set of rules as follows. The necessary coordinate system is defined in Figs. 1 and 8.

The **vp** vector:
Basically **vp** has a radial (vpr) and a downstream component (vpx). vpr will, as a default, be set negative in order to comply with observations from measurement. This will cause the spiral radius not to grow too rapidly. The downstream component vpx will be given a positive number in order to increase the spiral pitch in relation to pure BS application. A proposal for the **vp** components follows.

$$vp_x = kpx(\xi)\cdot vBS_x \qquad (a)$$
$$vp_y = kpr(\xi)\cdot vBS_y \qquad (b) \qquad (13)$$
$$vp_z = kpr(\xi)\cdot vBS_z \qquad (c)$$

Equations (13) define the artificial induction velocity vector components. These are based on the Biot-Savart genuine induction. It is assumed that only one trim parameter (*kpr*) is necessary for the components that are associated with the wake radial expansion. Separate is the longitudinal trim parameter (*kpx*) which can be used to increase or decrease the pitch of the tip vortex spiral. It is assumed that the trim parameters are functions of the *x* coordinate only. A first tentative attempt to predict a reasonable behavior of the trim parameters follows.

kpx should cause the initial pitch to be larger than that created with the Biot-Savart (BS) law only. In order to accomplish approximately a constant pitch of the spiral, the natural tendency of the BS law, to densify the spiral soon after birth, is counteracted by letting the *vpx* value be negative and numerically large at birth. Then the numerical value should diminish and then increase again at an *x* location where vortex breakdown takes place. At that position the absolute traveling velocity of the tip vortex should be close to the free stream velocity. A sketch of the principle of the *kpx* behavior is seen in Fig. 8. The complete curve is defined by 5 parameters. All of these can be manipulated in a corresponding computer code. Their proposed default values appear below.

Table 1

Parameter	Value
a	-.9
ξ_1	1.0
b	-.2
ξ_2	1.5
c	1.0

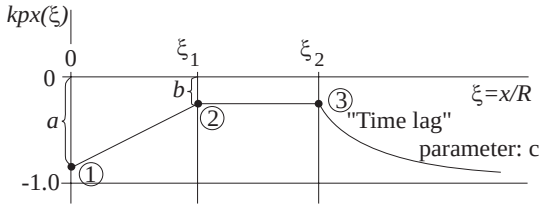

Figure 8

There are thus three intervals, see Fig. 8, where the *kpx* function needs to be defined. This is done as follows.

$$\text{1st interval}: kpx = a + \frac{b-a}{\xi_1}\xi \qquad (a)$$
$$\text{2nd interval}: kpx = b \qquad (b) \qquad (14)$$
$$\text{3rdinterval}: kpx = b + (-1-b)e^{c\cdot(\xi-\xi_2)} \qquad (c)$$

6. PREPARATIONS FOR A COMPUTER CODE ALGORITHM

The different regions, the different requirements on the filament elements etc must be dealt with in an organized way. At time zero there should be a choice between two possibilities. One choice is to run the case from scratch, i.e. there is no wake vorticity yet. The other choice is to use a previously generated wake and continue that case. The no-wake choice is described as follows.

At time step zero the motion of the blades and the simulated wind field are used to create wind vectors on the blade elements. The wind vectors are coordinate transformed to the different blade element local systems, whereby the angles of attack are obtained to be used for interpolation in the aerodynamic tables. This gives the aerodynamic coefficients, which are used to calculate the aerodynamic forces in N and Nm.

At time step one the wake vortices are first generated – only in Region 1 so far. This is accomplished by assuming that the aerodynamic circumstances at each blade element remains constant, as of step zero, during the time step dt. From the values of the lift coefficient C_L and the local wind speed, relative to the element, the corresponding bound circulation is directly calculated for every blade element. This generates a radial circulation distribution. From the circulation distributions it is possible to calculate the circulation of the trailing vortices as the difference in circulation between adjacent elements. The extent of the trailing vortices are assumed to be unaffected by induction in R1. Therefore the trailing elements extend from the bound circulation (or its trailing edge representation) to the position where that point was located at the previous time step, i.e. dt seconds ago. This is said with reference to the global coordinate system. The trailing vortex elements will, however, induce on the blade elements whereby the vector composition mentioned in step one is extended by summing up the Biot-Savart induction contributions from all trailing vortex filament elements – at each blade element. Thus, at each blade element there is now also an induction vector to be added to the previously mentioned local vector.

At time step 2 and at several more time steps the chain of events is identical to that described in the previous paragraph. The avoidance of any induction calculation at the R1 trailing vortices themselves is permissible as an approximation. The reason for the approximation is expediency of calculation. The background is that the wind normally blows through the rotor disk while the “downwash”, seeing the blade as an airplane wing, and the induction from the vortex filaments in the wake counteract the natural wind. This leads to the initial trailing vortices essentially staying in the disk plane. The approximation obviously becomes less valid the more the Region 1 vortices are extended azimuthally. A few chords corresponding to say 25 degrees of azimuth travel should be an acceptable extent of R1.

As the very first R1 trailing vortices reach the prescribed azimuth angle a new situation is created in the following time step. Here the oldest R1 vortices are grouped as indicated in Fig. 3 and 4. The grouping means two things. The newborn R2 vortex element gets its circulation from the sum of circulations of the oldest R1 vortex elements and the radial positioning is achieved through the technique condensed in Eq. (7). Meanwhile, in R1, the first vortex elements are discarded, a set of newborn elements is created and the rest of the R1 vortices remain fixed in the global system.

What has been said so far is valid for vortices emanating from the tip as well as from the root and if applicable from mid-blade as illustrated in Figs. 3 and 4.

When the number two and the following R2 vortices are created time stepwise, the process in R1 goes on as described while R2 is approaching its rear region border. When that happens the rearmost (oldest) R2 vortices of one full revolution (to be coined “spiral turn”) is discarded from R2 and suddenly replaced by an R3 “square”. This square, valid for one blade, is given the same length of circumference as the truncated R1 spiral turn equivalent circle circumference and the average circulation from all vortex filament elements that made up the spiral turn. Very soon after this creation of a square it is time to create the next representing the next blade etc. The center of the squares is given the average position and speed vector from averaging all positions and speeds of the elements making up the spiral turn.

The tilting of the square can be derived from the spiral turn as well. Both the center velocity vector and the tilt are maintained through the rest of the life of the squares.

To sum up the method in a few words it can be said that vortex elements (VE) are born into R1. They age and die at the end azimuth angle of R1 giving birth to R2 vortices, which drift with the wind and the induction from

all vortex elements. At the R2/R3 border their rearmost (in fact first and oldest) spiral turn is converted to a square and when the square has a certain number of generations, of squares following it, it dies too.

It seems suitable to describe the needs in the computer program for essential quantities. The following characteristics, pertaining to each vortex filament element node, need be preserved.

a. Circulation (One component)
b. Position (3 components)
c. Velocity (3 components)
d. Azimuth angle at birth (one comp.)
e. Time at birth (one comp.)

The node information will be based on three indices, one for blade individual, one for radial position (only in R2) and one for azimuth counter.

Finally it is mentioned that the procedures will have to depend extensively on coordinate transformations between the local blade element system and the global system.

7. INTERFACING WITH AERFORCE

AERFORCE is a Fortran subroutine package which is being used by aeroelastic computer codes, Ref. 5. The purpose of AERFORCE is to provide the calling program with external aerodynamic forces. These forces may then be used to drive the elastic motion of a structure such as a wind turbine. AERFORCE may alternatively be used in a pure aerodynamic performance program.

The interface of AERFORCE features a call to one single subroutine. This routine has a certain number of arguments selected to be the more mobile type, typically different from one time step to the next. AERFORCE consists of a number of subroutines that perform an internal communication among themselves using the *common* construct. Some of the *common* variables are also used by the calling routine. Parts of the described structure will have to be modified as described below.

The present text deals with the BEI method. Obviously several modifications will have to be made to the original AERFORCE code since it was created to serve the need for external load calculations using the BEM technique. Thus, the balance of momentum flux loss in the wake does not need to be employed in the BEI case. A natural modification seems to be that a mode switch be introduced. Setting this switch will either run BEI or BEM as dictated from input to the program. Also, when dynamic inflow will be used in BEM mode it will be excluded in the BEI mode. There are many more details to consider but the gist of the idea is to maintain the original capability of AERFORCE and augment it to include also the BEI technique.

8. TRIMMING THE MODEL USING EXPERIMENTS

8.1General Model Parameter - Needs for Trimming

The design of the BEI model includes several model parameters which can only be given reliable values through comparison with reality. Existing databases from wind tunnel tests with wind turbine models have the common affliction that the inflow velocities were not measured in any accurate way. This means that the hope lies with coming testing. At the time of writing the more promising test results seem to be provided by the MEXICO project, Ref. 8. But, before results will become available from the MEXICO tests there are possibilities in Sweden using a small wind turbine. This turbine is being used in testing off and on at the Royal Institute of Technology in Stockholm (KTH) in order to provide data of interest to a doctorial student. During the next few months it would be very useful to carry out some tests in support of the BEI model proposed above. The MEXICO tests already have a test matrix definition which will provide the data sought.

8.2 Finding the Angle of Attack in Testing

In previous testing, where no measurements of the inflow characteristics are available, but where the pressure distributions at several radial stations are available, the angle of attack α had to be achieved using theoretical methods. Two methods, known to the author, have been applied to this end.

The Pressure Signature Method
The pressure signatures in the vicinity of the stagnation point can be compared, from the tests with rotating rotor and from no rotation and/or testing of the two-dimensional airfoil in the wind tunnel. When the rotating signature agrees the most, between 3D rotating and 2D steady, it is concluded that the 2D α is the best estimate.

BEM Method
By assuming that the flux loss behind the rotor balances (equals) the thrust on the rotor it is possible to derive the reduction in the axial flow velocity through the disk. The balance equation then includes the Prandtl tip correction factor. α at the location of a blade may be derived from the geometry of the velocities of inflow, rotation and the local twist of the blade.

In e.g. Ref. 9 it was concluded that the BEM method gives too low an estimate of the angle of attack. The corresponding statement about the stagnation point could, however, not be made. The stagnation point method thus has an undetermined error bias. The two methods represent, however, what is possible to apply when good measurements are lacking. The importance of finding the angle of attack can be explained as follows.

Engineering performance methods rely on tabled aerodynamic information. This information is typically organized in four columns. They represent α, CL, CD and Cm respectively. From testing of instrumented wind turbines the pressure distributions around several blade sections may be available. By integrating the pressures the coefficients normal to the chord line (CN) and parallel with the chord line (Ct) may easily be computed. CL and CD are defined in a wind reference system while CN and Ct are in a system fixed to the physical blade cross section. The relationships between the coefficients are therefore a simple coordinate transformation as follows.

$$C_L = C_N \cos\alpha - C_t \sin\alpha \qquad (15)$$

$$C_D = C_N \sin\alpha + C_t \cos\alpha \qquad (16)$$

It can therefore be concluded that, if only the angle of attack were available, then CL and CD are immediately available according to Eqs. (15 and 16). It should be mentioned that Cm is the same in both systems and the CD value is lacking the contribution from friction. This lack can be made up for by some integral method of boundary layer computer code calculation which outputs the friction part. The most frequently used code XFOIL is of today's date free to fetch from the world wide web. It outputs the friction drag among many other quantities.

The described difficulty to obtain the angle of attack points to the necessity to measure the inflow velocity in testing. This requires a fast velocity or pressure sensor with the capability to capture the information upwind of and downwind of a blade. The idea is based on the simplified model of a blade in the form of a straight lifting line.

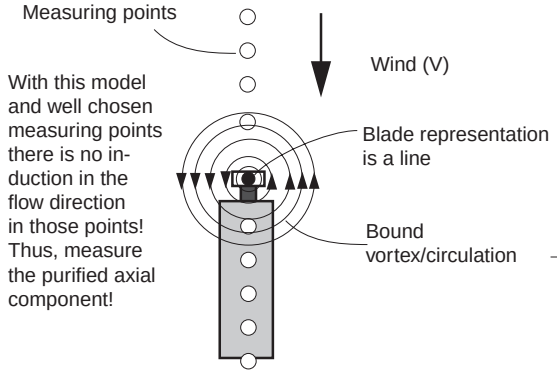

Figure 9

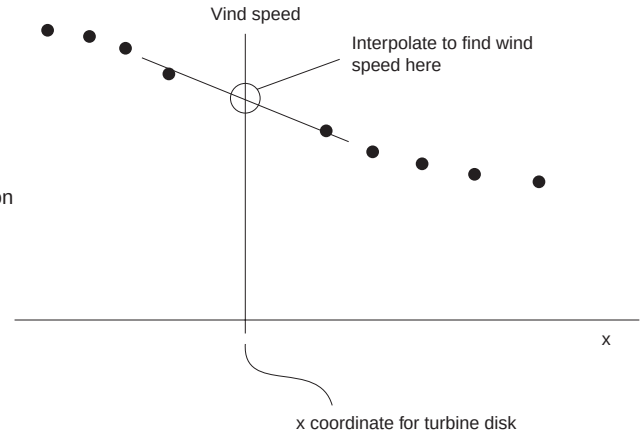

Figure 10

Fig. 9 shows a top view of a schematic nacelle of a wind turbine with one blade being vertical up. The lifting line model of a blade then appears as a dot – in the sketch it is the center of the circles. If the blade generates lift

around the particular radial position that is being studied then there is also circulation. If the measuring points are placed ahead of and behind the blade as shown, then the wind in the measured points would be free of any streamwise disturbance from the blade itself. The circulation would only contribute to lateral induced velocity components.

The wind, measured as described, can then be plotted versus the downstream coordinate x. Avoiding points very close to the turbine an interpolation for the turbine disk position can easily be made as indicated in Fig. 10. The interpolated value should be interpreted as the relevant axial velocity to be used for an evaluation of the angle of attack. This technique ascertains that the disturbance from the bound vorticity does not creep into the evaluation. The technique approaches the idealized 2D notion of the angle of attack definition.

The proposed scheme requires the fast velocity evaluation probe to be read only when it is exactly in front of and behind a blade. Repeated measurements must be carried out and all azimuth angle measurements must be filtered away except the one that fits the approved description. The test must also be repeated for several radial positions and the calculation as of Fig. 10 is repeated per radius.

The model idea is not perfectly reflected in the test setup. The errors/deviations of the theory are mainly due to three effects accordingly.

1. The distribution of chordwise vorticity is not in one point (in the Fig. 9 projection)
2. The finite blade thickness will cause a displacement disturbance (see the appendix)
3. The probe will interfere with the measurement causing a displacement effect

The described measuring method could be carried out with additional estimates of the errors caused by the three sources of error. Such analysis should accompany the presentation of the results from the measurement.

The angle of attack assessment technique as described is extremely important for evaluation of the measurements and for the model. Although important, that is not sufficient for the need to support a BEI model. For this purpose the trailing vortex pattern is equally important. The two parameter groups of paramount interest are the spiral geometry and the circulation strength. Both vary with the age of the vortices and this aspect must be considered in the design of the test matrix for an appropriate measurement definition.

9. REFERENCES

1."A Near Wake Model Compared with the Blade Element Momentum Theory"
Helge Aagaard Madsen and Flemming Rasmussen, Dep. of Wind Energy, Risø, Denmark
Proceedings from the conference: "The Science of Making Torque from Wind"
Delft Technical University, April 2004

2."Unsteady Airfoil Aerodynamics in Attached Flow on a Rotating Wind Turbine Blade"
Herman Snel, Netherland's Energy Research Foundation ECN, Wind Energy
Proceedings from the conference: "The Science of Making Torque from Wind"
Delft Technical University, April 2004

3."An Introduction to the Theory of Aeroelasticity"
Y. C. Fung
Dover Publications, New York, 1993

4."Insight into a Wind Turbine Stall and Post-stall Aerodynamics"
James Tangler, National Renewable Energy Laboratory (NREL)
1617 Cole Blv, Gloden, Colorado, USA

5."AERFORCE: Subroutine Package for Unsteady Blade Element/Momentum Calculations"
Anders Björck
The Aeronautical Research Institute of Sweden (FFA)
Rep.: FFA TN 2000-07

6. "Aerodynamik des Flugzeuges"
Schlichting & Truckenbrodt
Zweiter Band
Aerodynamik des Tragflugels ….
Springer-Verlag 1960

7. "Vortex System Studies on Small Wind Turbines"
Björn Montgomerie, Jan-Åke Dahlberg
Swedish Defence Research Agency, Aeronautics Division FFA
September 2003
Report number: FOI-R—0936--SE

8. European project: "Model Experiment in Controlled Conditions" (MEXICO), ENK6-CT2000-00309
Participants are: The Netherlands (coordinator), Greece, Denmark and Sweden.
Purpose: To run a 5 m diameter model turbine in the DNW biggest wind tunnel.
The blades are instrumented for pressure takings and Particle Velocimetry Imaging
will be applied for flow field mapping. Tunnel entry is expected 2004/2005.

APPENDIX
Flow Disturbance from a Two-dimensional Solid Body

1. Introduction

The background of the present text is the NREL database from the wind tunnel tests at the NASA Ames, California facility. A 10m diameter wind turbine was tested in the tunnel. One blade was instrumented with pressure holes and pressure probes mounted on the leading edge of the blade at five different radial positions. The tip of each probe had five holes designed to furnish information about the local flow angle and velocity. These probes were meant to help analysts evaluate the angle of attack for the pressure hole sections of the blade.

In an effort to evaluate the aerodynamic coefficients for the blade, the leading edge probe data are reproduced from the known conditions such as the wind speed in the tunnel, the rotational speed of the rotor and last, but not least, the pressure distribution on the blade.

The technique used in this evaluation is to initially conjecture the angle of attack. This allows a conversion from the aerodynamic coefficients for normal and tangential forces (CN and Ct) to the corresponding coefficients for lift and drag (CL and CD). In the next step the circulation on the blade is calculated and then the flow vector, at the probe tip, is calculated and compared with the measured vector. The error is used to guide the algorithm to produce a new angle of attack at the profile and then a new estimate of the probe tip flow vector follows and the iteration continues until a convergence criterion is satisfied.

The algorithm used to calculate the probe tip flow vector uses two modifications to the parallel oncoming flow, the circulation and the deviation of the flow caused by the solid body displacement. The method derived here is the solid body blockage effect in the blade profile section plane.

2. Aerodynamic Fundamentals

Fig. 1 shows the basic aerodynamic element of a point vortex, whose circulation is Γ. It is located at a point, that can be thought of as a vector *q*, and it effects any point in the xy plane by giving rise to an ”induced” velocity in any such point. *p* is an arbitrary point (position vector) where the induced velocity *v*, caused by the vortex, is evaluated. The Biot-Savart law of induction is used for this purpose. It assumes the following form where Γ, *p*, *q* and *v* are to be considered vectors in 3D space. The temporary extension to three dimensions is an expedient way to keep track of the induced vector direction.

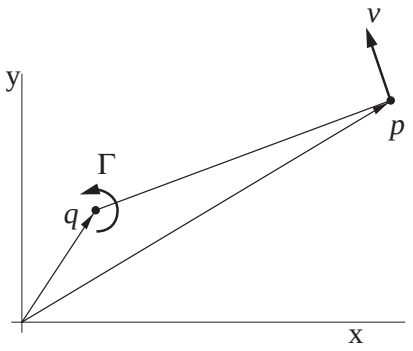

Figure 1

$$v = \frac{1}{2\pi d^2}\Gamma \times (p - q) \qquad (1)$$

Solving the determinant for vector cross multiplication, the resulting vector velocity components become

$$v_x = -\frac{\Gamma}{2\pi d^2}(y_p - y_q) \qquad (2)$$

$$v_y = \frac{\Gamma}{2\pi d^2}(x_p - x_q) \qquad (3)$$

The latter two expressions will be applied in the more complex context below. *q* will be associated with the location of the vortex while *p* will be the point of evaluation of the induced velocity.

3. Application to a Wing Profile

The induction calculation of the previous section is applied in a model of a 2D wing profile by choosing a number of points (q_i) on the circumference of the profile. At these points point vortices are applied. Initially these vortices are unknown as to their circulation strength. By evaluation of the induced velocity, in points mid-way between all q_i, and adding the ambient wind vector in these points a condition that the velocities are aligned with the profile surface leads to an equation system. From this system the unknown circulation strengths can be solved using Gaussian elimination.

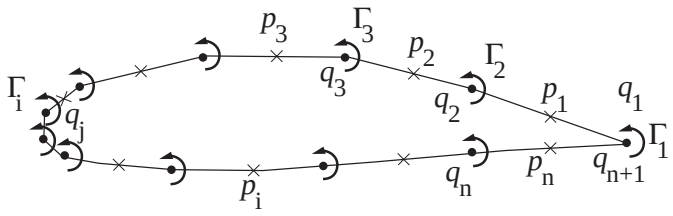

Figure 2

4. Equation Foundation

Once the circulations are known their influence anywhere in the plane can be directly calculated. This then applies to the tip of the pressure probe mentioned in the introduction. The induced vector field around this profile will become larger in error the more separated the suction side of the airfoil is.

With the model base of Fig. 2 the induced velocity in an arbitrary induction evaluation point *i* is

$$v_{x,i} = -\sum_{i=1}^{n} \frac{\Gamma_j}{2\pi d_{i,j}^2}(y_{p,i} - y_{q,j}) \qquad (4)$$

$$v_{y,i} = \sum_{i=1}^{n} \frac{\Gamma_j}{2\pi d_{i,j}^2}(x_{p,i} - x_{q,j}) \qquad (5)$$

Since the points of induction evaluation are placed mid-way between vortex points, the following expressions can be inserted in (4) and (5).

$$x_{p,i} = \frac{1}{2}\left(x_{q,i} + x_{q,i+1}\right) \qquad (6)$$

$$y_{p,i} = \frac{1}{2}\left(y_{q,i} + y_{q,i+1}\right) \qquad (7)$$

The quantity $d_{i,j}$ is the distance from q_j to p_i. It is obtained from the Pythagorean theorem as follows.

$$d_{i,j} = \sqrt{\left(x_{q,j} - x_{p,i}\right)^2 + \left(y_{q,j} - y_{p,i}\right)^2} \qquad (8)$$

Also the expression (8) need to be inserted in (4) and (5) before summation.

The sum of induction contributions from all vortices, at say p_i, is called v_i. But, also the free stream velocity is superimposed on v_i.

5. Equation Details

From the beginning all vortices are unknown as to their circulation strength. These strengths must be solved from a set of equations that are based on the condition that the induced vector plus the free stream vector be parallel to the surface – or, in fact, an approximation for the surface. Fig. 3 shows one panel of the profile. The induced vector on this panel, together with the free stream vector will be set to be parallel with the line defined by the points q_i and q_{i+1}, although the connection between the two points is generally a curve, not a straight line. This approximation is

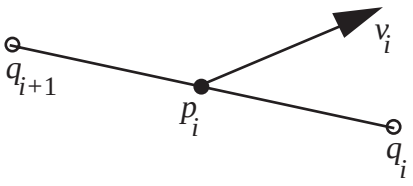

Figure 3

accepted in this model. It may possibly invite significant errors at the leading edge of the profile because of the high curvature of the surface contour at that location. The cure is to place check points more densely in that region. The flow alignment condition can be formulated as follows.

The total velocity, i.e. $V_{\infty,i} + v_i$, at p_i is in alignment with the surface when

$$(V_{\infty,i} + v_i) \times (q_{i+1} - q_i) = 0 \tag{9}$$

The cross product can be obtained from evaluation of a determinant.

$$\begin{vmatrix} \hat{x} & \hat{y} & \hat{z} \\ V_{\infty,x} + v_{x,i} & V_{\infty,y} + v_{y,i} & 0 \\ x_{q,(i+1)} - x_{q,i} & y_{q,(i+1)} - y_{q,i} & 0 \end{vmatrix} = \begin{Bmatrix} 0 \\ 0 \\ -\left(y_{q,i} - y_{q,i+1}\right)\left(v_{x,i} + V_{\infty,x}\right) + \left(x_{q,i} - x_{q,i+1}\right)\left(v_{y,i} + V_{\infty,y}\right) \end{Bmatrix} \tag{10}$$

Here $\hat{x}, \hat{y}, \hat{z}$ are unit vectors. Obviously the two-dimensional vectors seen in Fig. 3 have been extended to three dimensions. The result from evaluation of the determinant is thus a vector perpendicular to the surface in Fig. 3. But, this result is only used to be set to zero, which will create the relationships necessary for the set of equations required. Thus from (10), for the surface interval *i*, we have the equation

$$\left(x_{q,i} - x_{q,i+1}\right)\left(v_{y,i} + V_{\infty,y}\right) - \left(y_{q,i} - y_{q,i+1}\right)\left(v_{x,i} + V_{\infty,x}\right) = 0 \tag{11}$$

In anticipation of later needs this should be written

$$\left(x_{q,i} - x_{q,i+1}\right)v_{y,i} - \left(y_{q,i} - y_{q,i+1}\right)v_{x,i} = -\left(x_{q,i} - x_{q,i+1}\right)V_{\infty,y} + \left(y_{q,i} - y_{q,i+1}\right)V_{\infty,x} \tag{12}$$

Inserting (4) and (5) in (12) gives for the *i*:th interval, with induction contributions from all vortex points (*j*), the following expression.

$$k_{i1}\Gamma_1 + \ldots + \frac{-\left(y_{p,i} - y_{q,j}\right)\left(y_{q,i+1} - y_{q,i}\right) - \left(x_{p,i} - x_{q,j}\right)\left(x_{q,i+1} - x_{q,i}\right)}{2\pi\left\{\left(x_{p,i} - x_{q,j}\right)^2 + \left(y_{p,i} - y_{q,j}\right)^2\right\}}\Gamma_j + \ldots\ldots + k_{in}\Gamma_n =$$

$$\left(x_{q,i+1} - x_{q,i}\right)V_{\infty,y} - \left(y_{q,i+1} - y_{q,i}\right)V_{\infty,x} \tag{13}$$

There are *n* such equations, one for each panel mid-point *i*. Eq. (13) represents a system of equations that can be written as follows.

$$\mathbf{K} \cdot \mathbf{\Gamma} = \mathbf{R} \tag{14}$$

where

$$\mathbf{K} = \begin{bmatrix} k_{11} & k_{12} & . & k_{1j} & k_{1n} \\ & . & & & \\ & & . & & \\ & & & . & \\ k_{n1} & . & . & . & k_{nn} \end{bmatrix} \quad \text{and} \quad \mathbf{\Gamma} = \begin{Bmatrix} \Gamma_1 \\ \Gamma_2 \\ \ldots \\ \Gamma_j \\ \Gamma_n \end{Bmatrix} \tag{15}$$

R is also a vector whose typical element is seen as the right member in Eq. (13). Eq. (14) is a straight-forward linear system which can be solved for the $\mathbf{\Gamma}$ values using Gauss elimination. The typical k_{ij} element is the busy looking term to the left of the equality sign in Eq. (13).

6. Application

The result from the steps of derivation described above is a set of discrete circulation strengths (Γ) placed as seen in Fig. 2. The strengths are constrained to give a flow that is parallel to the surface of the profile. But, there is no Kutta condition. The total circulation, i.e. the sum of the individual circulation strengths, turns out not to be zero in the general case. Since the program was generated for the exclusive purpose of providing a body displacement velocity vector, in an arbitrary point outside the airfoil, it should not produce any lift. Therefore no net lift should be generated by the vortices, which means that the sum of circulations should be zero except for insignificant decimal roundings. A method to eliminate the residual lift appears below.

The usefulness of the solution lies in its capability to be used for induction calculation outside of the profile itself. This can be used to estimate the disturbance velocity vector at the position of a probe. Such probes were part of one of the blades on the NREL test wind turbine in the NASA Ames test activity. The analysis of the corresponding test data is in fact the reason for this text. Since the Kutta condition is no part of this analysis, the disturbance, calculated for the probe positions, represents a solid body disturbance without lift effects. The lift effects will have to be provided from other methods. The disturbance can, however, be calculated for any angle of attack. In the application of the program this possibility was utilized.

The equations and the necessary Gaussian elimination, to obtain the Γs, were implemented in a Fortran program. The program was used as one of several tools in the analysis of the NREL test data. For reasons to eliminate the residual lift, it turned out to be practical to manipulate the y coordinate of the first point given (yTE), see Fig. 4. By increasing/changing this value, wagging the tail as it were, the net circulation can be decreased/changed until the total circulation becomes zero. The corresponding geometric deformation appears in Fig. 4. The case definition input routine provides the user with a relatively expedient method to accomplish this goal. Zero lift is thus accomplished by running the program several times and setting the yTE parameter to values governed by the learning from the previous iterations. At further utilization of the computer program the search for zero net lift should be implemented as an automatic feature in the code itself.

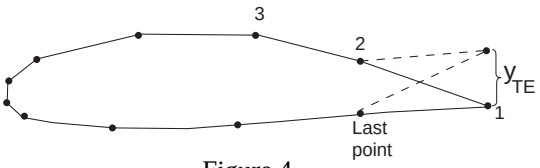

Figure 4

In running the program the point of evaluation, representing the probe position in the NREL tests, was positioned at: x = -0.8 and y = -.1. At a locally felt velocity of 11 m/s, at the 30% chord point, the disturbance velocity at x,y was about 0.2m/s. This disturbance should also be compared to the corresponding lift induced velocities at the same point. The latter were of order of magnitude of 1.5m/s at 8˚ angle of attack. In summary the displacement disturbance is 13% of the typical lift induced velocity at "normal" operation. The lift induced disturbance was calculated as Biot-Savart induced velocity from a single vortex located at a fraction of chord, which was obtained as Cm/CN. The latter two quantities were directly available from the NREL tests.

Since the method is perfectly inviscid the flow velocity V, which is an input, results in a strength, for the set of vortices, which is directly proportional to V. The induced velocity components (vx,vy) at the point of evaluation (x,y) are also directly proportional to the vortex strength and V. So, by calculating (vx,vy) for a series of angle of attack (α) values, while V was held constant at 10 m/s, a useful database was obtained for all blade profiles that were instrumented in the NREL tests. If e.g. the local velocity were to be say 8 m/s, the (vx,vy) values in the database would be multiplied by 8/10. The database is reproduced below, see diagram in Fig. 5 and the table.

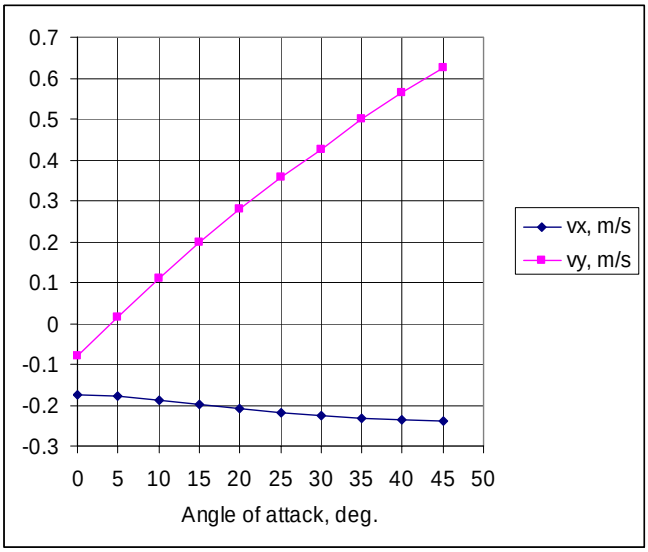

Figure 5

Table - database

Probe coordinates:

xA =	-0.8	yA =	-0.105
Vlocal =	10	m/s	

alpha	vx, m/s	vy, m/s
0	-0.176	-0.081
5	-0.179	0.016
10	-0.187	0.11
15	-0.198	0.197
20	-0.208	0.28
25	-0.218	0.359
30	-0.225	0.424
35	-0.231	0.499
40	-0.236	0.565
45	-0.238	0.626

7. Accuracy

The simple inviscid flow model described above does not represent the disturbance of the flow field well in case of heavy separation. For such cases the contour of the model should encompass also the separated flow region borders. It was, however, judged that since the correction from the solid blockage is very small, a correction on the correction would not be worth the effort of running additional forms of separated flow representation. The effect was therefore ignored.

Another fact that should be considered is that the method is two-dimensional, i.e. the wing has infinite extent into and out of the plane of the paper (with reference to Fig. 2). Thus, near the tip and the root of the blade the the “wing” is only half infinite. Therefore the disturbance velocity should be halved at these positions and a transition from this half to full effect at mid-blade should be considered.